Pure & Appl.Chem., Vol.54, No.12, pp.2307-2315, 1982.
Printed in Great Britain.

0033-4545/82/122307-09$03.00/0
Pergamon Press Ltd.

EXAFS SPECTROSCOPY OF COORDINATION COMPLEXES IN NON-AQUEOUS SOLUTIONS

J. Goulon* and C. Goulon-Ginet

Laboratoire de Chimie Théorique, ERA n°22 du CNRS, Université de Nancy I, B.P. 239, 54506 Vandoeuvre-lès-Nancy, France,
et
Laboratoire pour l'Utilisation du Rayonnement Electromagnétique, Laboratoire Propre du CNRS associé à l'Université de Paris-Sud, 91405 Orsay, France.

Abstract - This paper is reviewing a number of recent studies carried out at LURE concerning the formation, in non aqueous solutions, of molecular complexes $(LiBr)_n$, $(MBr_4^{2-})_q$, $[ZnCl_p(selenourea)_q]$ and the complexation of rubidium or strontium cations by various macrocyclic ligands: 2-2-2-cryptand, 18C6 or 15C5 crown ethers, and natural ionophores such as calcimycin (A23187) or lasalocid (X-537A).

INTRODUCTION TO X-RAY ABSORPTION SPECTROSCOPY OF SOLUTIONS

In the recent years, the advent of synchrotron radiation emitted by e^+/e^- storage rings has considerably renewed the interest in X-ray absorption spectroscopy, as for the first time, very intense, white beams of X-ray photons were available (1-4). Further advances , either in the design of new machines especially dedicated to synchrotron radiation emission or in the technology of powerful wigglers are still to be expected. Thus, one may guess that many experiments in the field of solution chemistry which are to-day time consuming will doubtless become easier in the near future.

There are two distinct but complementary aspects of this spectroscopy :
(i) The details of the X-ray absorption near edge structure (XANES) can be very helpful in ascertaining the oxidation state or the site symmetry of metal centers in complexes or clusters (5,6).
(ii) The small modulation of the absorption coefficient above an absorption edge commonly referred to as EXAFS (Extended X-ray Absorption Fine Structure) has a structural content related to the radial distribution of the different atoms surrounding the absorbing center (7).

Indeed this fine structure (EXAFS) has been known for a long time, as it was discovered by Kronig (8) early in this century. However its potentiality as a structural tool was recognized rather recently by Stern et al. (9,10) who developed the theoretical background required for a quantitative analysis of the phenomenon. According to the Fermi's golden rule, the probability for a X-ray photon to be absorbed by a core electron depends on both the initial and final states of the excited photoelectron. The initial state is a localised deep core level defining a very selective absorption edge (K or L) whereas the final state has to be represented by the interference of an outgoing photoelectron spherical wave with an incoming wave resulting from the backscattering of this photoelectron by each neighbouring atom. This energy dependent interference process gives rise to the observed modulation of the absorption coefficient on varying the photon energy. As far as the EXAFS signal can be resolved into individual contributions of j shells of N_j equivalent scattering centers, then the period of the EXAFS oscillations will be related to the absorber/scatterer interatomic distance R_j . The amplitude of these oscillations will be directly proportional to N_j, but it will depend on the nature of the scattering element and also will be sensitive to any disorder affecting the relative distance R_j. Furthermore, as these photoelectrons exhibit a rather short coherence length, the EXAFS oscillations can only be representative of the short range ordering (i.e. $R_j < 5$ Å) around the absorber : only local structural information can be gained from this technique which however is quite versatile in that it can be used in solutions or in amorphous systems as well as in polycrystalline samples. As the K- or L-edges of the various elements are well separated by hundreds of eV, both techniques (XANES/EXAFS) are inherently selective for a given absorbing element and impurities are usually not interfering. However, these techniques cannot be selective of a given site of the absorbing element and this is a severe limitation when complex systems are investigated such as metalloproteins, or when dealing with mixed species in solution.

The sensitivity of absorption measurements is strongly dependent on the energy of the X-ray photons : soft X-rays (e.g. $E < 5$ keV) are dramatically absorbed by the solvent or any kind of window materials, and as a consequence, most of the EXAFS studies on solutions performed at LURE (Orsay) concern rather high energy edges ($E > 7$ keV). However, the sensitivity of the XANES/EXAFS measurements can be enhanced for dilute systems by detecting the X-ray fluorescence emission of the sample at right angle to the incident beam : this method removes the background absorption of the solvent, thereby increasing the sensitivity (2,11).

Solution chemistry applications of EXAFS are mostly concerning aqueous solutions and thus, fall outside the topics covered by this meeting (12-18). This restriction is also excluding practically all EXAFS studies of metalloproteins. Indeed, there are only very few of the EXAFS papers dealing with non aqueous solutions (19-21). In this paper, we wish however to illustrate the potentiality of this technique by reviewing a number of recent studies carried out at LURE (the french synchrotron radiation center) concerning the formation of molecular complexes $[LiBr]_n$, $[MBr_4^{2-}]_q$ (M = Co, Cu, Zn), $[ZnCl_p(selenourea)_q]$, and the complexation of Rb^+ or Sr^{2+} ions by various macrocyclic ligands. Other studies involving metal ammonia solutions or Ziegler-Natta catalysts are still in a stage of development and are not to be discussed here.

ANALYSIS OF THE EXAFS SPECTRA

The analysis of the spectra includes the usual "preparation" of the data, i.e. (i) removal of the pre- and post-edge background contribution to the whole absorption coefficient $\mu(E)$ by a fast smoothing procedure, (ii) normalization of the spectra with respect to the edge jump, (iii) transformation from the photon energy scale to the photoelectron wave scale $k = [(2m_e/\hbar^2)(E-E_o)]^{1/2}$ which implies the definition of the energy threshold E_o above which the photoelectron is free. For a discrete gaussian distributed lattice, the normalized oscillatory component $\chi(k)$ of the absorption coefficient is given by the approximate EXAFS formula :

$$\chi(k) = \frac{1}{k} \sum_j \frac{N_j}{R_j^2} \exp(-2\sigma_j^2 k^2) \, |F_j(k,\pi)| \, A(R_j,k) \sin[2kR_j + \psi_j(k)] \qquad (1)$$

where $F_j(k,\pi)$ and $\psi_j(k)$ denote respectively the backscattering amplitude and the total phase shift for the jth shell, whereas σ_j^2 is the mean squared relative displacement of the absorber/scatterer pair from the distance R_j. Neither the analytical formulation of $\chi(k)$ given in equation (1) nor the parametrization of the functions $F_j(k,\pi)$ and $\psi_j(k)$ proposed by Teo and Lee (22) on the basis of pseudo ab initio calculations are fully satisfactory from a theoretical point of view but it is now well recognized that quite reliable distances can be determined within these approximations as long as one keeps slightly adjustable the energy offset E_o involved in the definition of k : e.g. the possible effect on $\psi_j(k)$ of the cationic charge states can thus be compensated by a slight shift of E_o. The prediction of the EXAFS amplitude is not yet fully satisfactory, even if equation (1) is corrected in order to take into account the finite energy resolution of the monochromator as discussed by Lengeler and Eisenberger (23) and other experimental limitations such as the effects of harmonics at the output of the monochromator (24). A major difficulty is the evaluation of the factor $A_j(k)$ accounting for the loss of coherence of the photoelectron due to inelastic processes (25) and tentatively written as : $A_j(k) = S^2(k) \exp(-2\Gamma_j R_j/k)$ where :

$S^2(k) = [(S_o^2-1)/\pi] \arctan[(k-k_s)\alpha] + (S_o^2+1)/2$, S_o^2, k_s and α being predetermined fixed parameters which can be transferred from one system to the other without major change ($0.7 < S_o^2 < 0.8$, $k_s = 9$ Å^{-1} , $\alpha \simeq 7$ Å). Γ_j has to be adjusted more carefully e.g. using model compounds for which the Debye-Waller term can be evaluated from vibrational spectroscopy (21).

The Fourier transformed spectra $\tilde{\chi}_j(R)$ reproduced in this paper are all corrected for the phase shifts and amplitude of the dominant shell j according to :

$$\tilde{\chi}_j(R) = \int_0^\infty dk \; g(k) \; \chi(k) \; \frac{R_j^2 k}{N_j F_j A_j} \exp\left[2\sigma_j^2 k^2 - 2ikR - i\psi_j(k)\right] \qquad (2)$$

where g(k) is a symmetrical Kaiser window function minimizing the side lobes of the FT signals. When practicable, we thus use the Lee-Beni criterion of coincidence of the maxima of $|\tilde{\chi}_j(R)|$ and $\mathrm{Im}\,\tilde{\chi}_j(R)$ in order to fix E_o (26).

It is also often desirable to refine the amplitude parameters (N_j,σ_j) and we have been led to develop a package of fast but safe fitting routines, as well as simulation routines of the EXAFS oscillations assuming known structural parameters. The fitting procedures always require to reduce as much as possible the number of independent parameters because of well-known correlation effects. Fourier filtering in the R-space is of common practice for reducing the number of contributing shells. Reference to model compounds is also helpful for fixing amplitude parameters.

DETECTION OF INORGANIC CLUSTERS IN SOLUTION

In a recent study (21), we were able to detect by EXAFS the formation of tetrameric species $[LiBr]_4$ in diethylether (Et_2O), but only of dimers $[LiBr]_2$ in diethylcarbonate (DEC), in perfect agreement with our predictions inferred from the colligative properties of these solutions, from dielectric measurements as well as from vibrational spectroscopy. The EXAFS spectra were recorded at the bromine (Br*) K-edge using as a reference a dilute solution of CBr_4 in Et_2O. Further work on Li_2ZnBr_4, Li_2CoBr_4 and Li_2CuBr_4 solutions in Et_2O led to EXAFS spectra quite consistent with the formation of tetrahedral units MBr_4^{2-} which are strongly distorted in the case of the Li_2CuBr_4 solution due to the presence of a strong Jahn-Teller effect. However, when the stoechiometric ratio [Br]:[Zn] becomes less than 4 (e.g. for a $LiZnBr_3/Et_2O$ solution), the average number of bromine atoms around a zinc atom remains of the order of 4, each bromine being bound (in average) to two zinc atoms: our result thus favours the presence of multimeric species $[LiZnBr_3]_q$ comparable to those observed for the crystal structure of $CsCuBr_3$ (27). It is also well known from cryoscopic data (28) that $ZnBr_2$ in dimethylcarbonate should form multimeric species $[ZnBr_2]_q$, q increasing steeply with concentration. This result is obviously supported also by a recent EXAFS study of $ZnBr_2$/ethylacetate solutions carried out at LURE by a different group of workers (20) who concluded to the presence of quasi lattice structures. As far as we are concerned, we never observed in our EXAFS spectra any indication that the solvent (Et_2O or DEC) was participating to the coordination of the metal.

We intend in the following to detail somemore new results relative to the formation of complex species $ZnCl_p[selenourea]_q$ in methanolic (MeOH) solutions. Urea, thiourea, selenourea and related derivatives such as semicarbazides have been known for many years to be strong complexing agents of metals, some of these complexes being formerly used as analytical tools (29-31). The K-absorption edge of selenium falling in a very convenient energy range for an EXAFS investigation, selenourea (SeU) appeared to us as an attractive, commercially available ligand. Its poor natural stability required us to recrystallise it shortly before use and to add traces of a stabilising agent i.e. hydroquinone (32) to the prepared solutions which were stored in the dark.

For the sake of comparison, we have reproduced in Fig. 1a the FT-spectrum $\tilde{\chi}_1(R)$ of pure powdered selenourea, whereas Fig. 1b presents the FT-spectrum $\tilde{\chi}_1(R)$ of a selenourea/MeOH solution (0.2 M). The phase shifts and amplitude parameters injected into equation (2) were those relevant for a Se*...N pair. The average intramolecular distances Se*...C = 1.90 ± 0.02 Å and Se*...N ≃ 2.7_5 ± 0.0_3 Å derived from these spectra compare reasonably well with the crystallographic data of Rutherford and Calvo (33), the crystal exhibiting up to 9 unequivalent selenium sites with a rather large distribution of the distances Se...C and Se...N. The major difference between the spectra 1a and 1b is a severe reduction in Fig. 1b of the broad, unresolved contribution of intermolecular distances Se...N, Se...Se ($3.3 \leqslant R \leqslant 4.3$ Å) which however does not vanish totally, thus suggesting strong solute-solute or solute-solvent interactions.

Figure 2a is displaying the (Se*) FT-spectrum $\tilde{\chi}_2(R)$ obtained for a mixture in equal proportions of the previous selenourea/MeOH solution (0.2 M) with an anhydrous $ZnCl_2$/MeOH solution (0.1 M). Clearly the strong additional signal peaking at 2.47 Å is to be assigned to a high Z scatterer, i.e. to a Se*...Zn shell. As we injected into equation (2) the amplitude and phase-shift parameters pertinent to such a Se*...Zn shell, the peak position gives the right Se*...Zn distance which compares very well with distances Se...Zn found in other complexes (34). On Fourier filtering the partially resolved contributions of the shells Se*...Zn and Se*...N, we obtained the agreement displayed in Fig. 2b. The only parameters permitted to vary were respectively the average numbers of zinc ($N_2 = 1.0 \pm 0.2$) and nitrogen ($N_3 = 2.1 \pm 0.2$) the distance Se...Zn ($R_2 = 2.46 \pm 0.02$ Å) and the corresponding mean squared displacement $\sigma_2 = 0.081$ Å , reference being made to previously analysed data for presetting the other parameters.

Further information is to be gained from the EXAFS spectrum recorded at the zinc K-edge. The FT-spectrum $\tilde{\chi}(R)$ reproduced in Fig. 3a was obtained on selecting for equation (2) the amplitude and phase-shift parameters corresponding to a Zn...Cl shell. Indeed the Zn*...Cl and Zn*...Se contributions are not resolved but if we notice that the respective scattering phase shifts of Cl and Se differ from π radians, then a careful examination of the phase of $Im\tilde{\chi}(R)$ definitively supports the presence of these two components. A two shell fit of the filtered signal back-transformed in the k-space proved to be rather successful as illustrated by Fig. 3b. Again a restricted number of parameters was left free to vary : the average number of chlorine ($N_1 = 3.5 \pm 0.5$) and selenium ($N_2 = 1.9 \pm 0.2$), the distance Zn...Cl ($R_1 = 2.26 \pm 0.03$ Å) and the relevant value of σ_1 ($\simeq 0.07_5$). The distance Zn...Se and the corresponding relative displacement σ_2 were directly taken from the data analysed at the selenium edge.

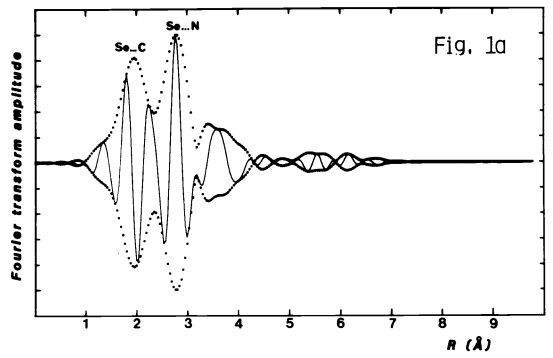

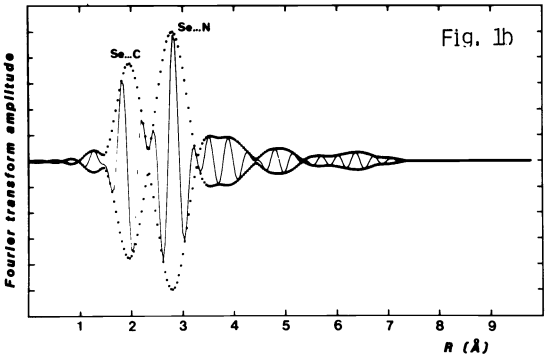

Fig. 1a. Imaginary part (full line) and absolute value (dotted line) of the Fourier transformed EXAFS spectrum at the selenium K-edge for pure powdered selenourea. The calculations include the corrections of the amplitude and phase-shifts for a Se*...N pair.

Fig. 1b. EXAFS corrected pseudo-radial distribution $\tilde{\chi}_1(R)$ for a selenourea solution in methanol (0.2 M) at the selenium K-edge.

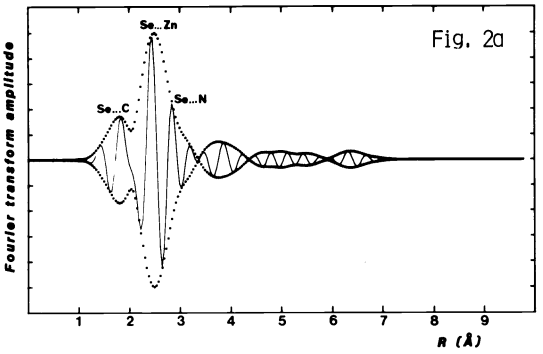

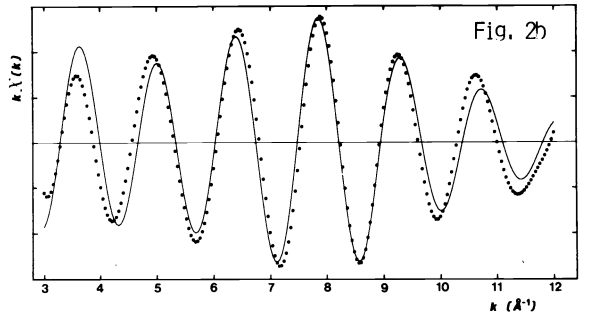

Fig. 2a. EXAFS corrected pseudo-radial distribution $\tilde{\chi}_2(R)$ for a mixture v/v (1:1) of a selenourea/MeOH solution (0.2 M) with a $ZnCl_2$/MeOH solution (0.1 M) at the selenium K-edge.

Fig. 2b. Fourier backtransformed data (dotted line) and best nonlinear least-squares fit (full line) of the spectrum 2a for a two shell contribution of Se*...Zn and Se*...N.

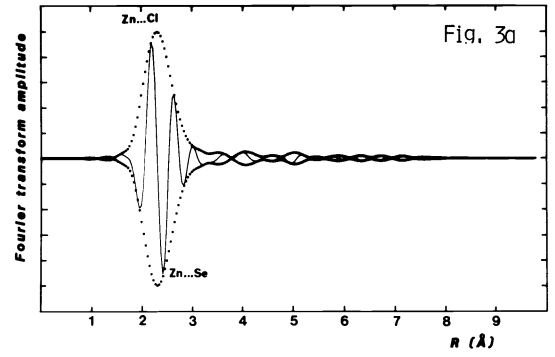

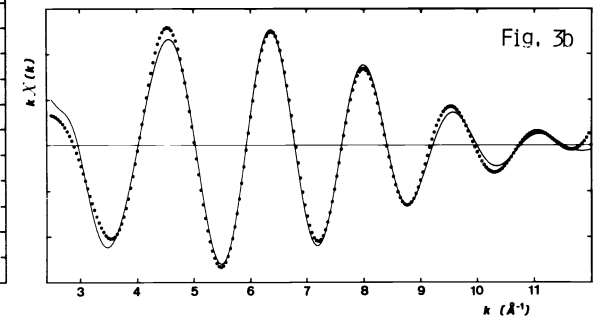

Fig. 3a. EXAFS corrected pseudo-radial distribution $\tilde{\chi}(R)$ for a mixture v/v (1:1) of a selenourea/MeOH solution (0.2 M) with a $ZnCl_2$/MeOH solution (0.1 M) at the zinc K-edge.

Fig. 3b. Fourier backtransformed data (dotted line) and best nonlinear least-squares fit (full line) of the spectrum 3a for a two-shell contribution of Zn*...Cl and Zn*...Se.

These results cannot be understood if we postulate the existence in the solution of only $ZnCl_4^{2-}$, $ZnCl_2[SeU]_2$ or even $ZnCl_2[SeU]_4$ species. Indeed $MCl_2[SeU]_2$ and $MCl_2[SeU]_4$ complexes have been isolated in the solid phase for $M = Co^{2+}$ (35) whereas the crystal structure of the sulfur analogs $ZnCl_2[thiourea]_2$, $CoCl_2[thiourea]_2$, $CoCl_2[thiourea]_4$ have been elucidated for many years (36-38). On the basis of our EXAFS data, we would merely postulate the formation of polymeric aggregates $[ZnCl_2[SeU]_2]_q$, the chlorine atoms being coordinated to two zinc atoms like in $ZnCl_2$ or $ZnBr_2$ solutions. Starting from tetrahedral subunits $[ZnCl_4]$, we suggest that the selenium atoms might approach the zinc atom from anyone of the free apexes of the corresponding cc lattice, chemical exchange of the chlorine/selenium mixing the respective positions of these atoms. If we accept this model, we may perfectly assign the broad band peaking at 3.8 Å in Fig. 2a to unresolved Se...Se and Se...Cl distances (expected distances for tetrahedral bonding being respectively 4.0 Å and 3.7 Å).

Anyway, the EXAFS spectra clearly confirm that the coordination of selenourea involves the selenium atom and not the nitrogen atoms although $ZnCl_u(NH_3)_v$ complexes are well known (39). This is in perfect agreement with the crystal structure of $ZnCl_2[thiourea]_2$ (36). The slightly shorter distance Zn...Cl found by EXAFS is however more consistent with the distances found in $(NH_4)_2ZnCl_4$ for the tetrahedral unit $ZnCl_4^{2-}$ (40).

COMPLEXATION OF Rb^+ AND Sr^{2+} BY MACROCYCLIC IONOPHORES.

The complexation of alkali and alkaline-earth cations by macrocyclic ligands has been matter of considerable interest since it was recognised that several natural compounds (e.g. valinomycin) acted as ionophores through biological membranes. The use of these macrocyclic ligands is now widespread and areas of applications (41) include the selective complexing of cations, the extraction and purification of metals, phase transfer catalysis, anionic polymerisation and dissolution of otherwise insoluble salts in solvents of low polarity. The structure in solution of complexes of variable stoechiometry (1:1 or 1:2) is still an open question which deserves further studies as shown below. For the sake of convenience of X-ray absorption measurements, Rb^+ and Sr^{2+} cations were preferred to K^+ and Ca^{2+} as the K-edge of the latter falls in the soft X-ray energy range where solvents become highly absorbing.

Complexation of rubidium ions.

We shall consider first the complexation of rubidium ions by crown ethers featuring a different radius r_c of the macrocyclic cavity : 15-C-5 ($0.86 < r_c < 0.92$ Å) and 18-C-6 ($1.34 < r_c$ 1.43 Å), reference being also made to the (2-2-2)cryptand. We also varied the nature of the counter-ion (NCS^-, Br^-, CO_3^{2-} and the bulky non coordinating tetraphenylborate BPh_4^-) as well as the nature of the solvent : pyridine ($\varepsilon = 12.5$, of strong basicity), MeOH ($\varepsilon = 33$, hydrogen bonding) and nitromethane $MeNO_2$ ($\varepsilon = 39$, disrupting ion pairs).

As a reference, we have reproduced in Fig. 4a the FT-spectrum $\tilde{\chi}_1(R)$ of a powdered sample of $[Rb^+:(2\text{-}2\text{-}2)\text{cryptand}],Br^-$. The amplitude and phase-shift parameters used in equation (2) were those of a Rb*...O shell, as obviously the dominant signal of the spectrum is to be assigned to the coordination shell (6 oxygens and 2 nitrogens) at an average distance $R_1 = 2.92 \pm 0.03$ Å, the second peak being due to the 18 equivalent carbons of the lipophilic cage at $R_2 = 3.75 \pm 0.03$ Å (41). It is noteworthy that the distance Rb...Br is probably exceeding 6 Å because we did not observed any significant difference in the spectrum when CO_3^{2-} ions replaced the Br^- anions.

The spectrum $\tilde{\chi}_1(R)$ obtained for a solution of $[Rb^+:(2\text{-}2\text{-}2)\text{cryptand}]BPh_4^-$ in pyridine (0.15 M) shown in Fig. 4b was rescaled and thus does not make apparent an overall reduction of the amplitude of the first peak by a factor of 1/3. We understand this reduction as a consequence of the lower rigidity of the cage in solution. This effect is even more spectacular for the Rb...C shell : there is an apparent broadening of the corresponding signal, the amplitude of which is reduced by a factor of $\sim$1/2. One should also notice the presence of a shoulder peaking at 4.3 Å which is not noise since we observed it, with the same phase, whatever the solvent or the anion was.

We next have recorded the EXAFS spectra of two solutions of $[Rb^+:(15\text{-}C\text{-}5)_n]BPh_4^-$ in pyridine varying the ratio $r = [\text{ligand}]/[\text{ion}]$ from 1.8 to 5.6 . The two FT-spectra $\tilde{\chi}_1(R)$ reproduced in Fig. 5a and Fig. 5b would perfectly superimpose each other up to 6 Å and exhibit exactly the same amplitude. However, as illustrated by Fig. 5a, the amplitude of the first peak does not exceed the two third of the amplitude of the Rb...O,N signal observed for the solution of $[Rb^+:(2\text{-}2\text{-}2)\text{cryptand}]BPh_4^-$. Again noteworthy is the existence of a second, intense signal peaking at 4.2_5 Å but with an inverse phase.

Also shown in Fig. 6a and Fig. 6b are the FT-spectra $\tilde{\chi}_1(R)$ obtained for two solutions of $[Rb^+:(18\text{-}C\text{-}6)_n]BPh_4^-$ in pyridine corresponding respectively to $r = 1.1$ and $r = 6$. Unexpectedly a quite significant reduction of the amplitude of the peaks Rb...O ($R_1 \simeq 2.92$ Å) and Rb...C ($R_2 \simeq 3.8$ Å) is observed when r is increased. Again a strong signal featuring an inverse phase is found at 4.2_5 Å which partially overlaps the less intense signal Rb...C at 3.8 Å.

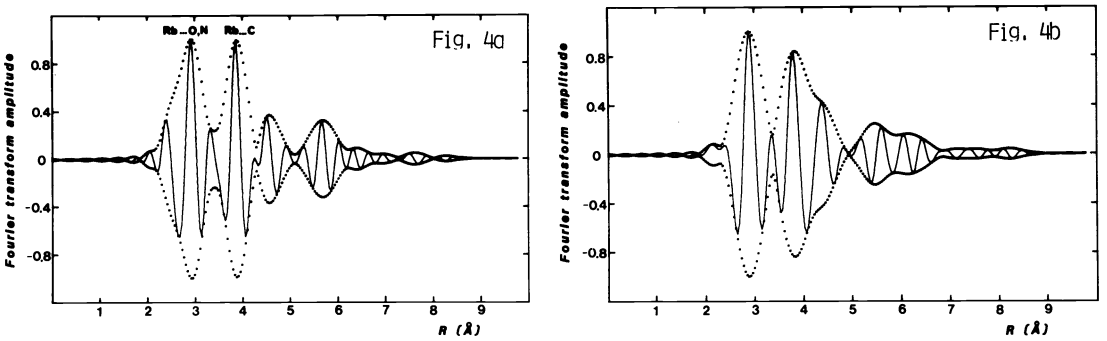

Fig. 4a. EXAFS corrected pseudo-radial distribution $\tilde{\chi}_1(R)$ for a powdered sample of $[Rb^+:(2\text{-}2\text{-}2)\text{cryptand}]Br^-$ at the rubidium K-edge.

Fig. 4b. EXAFS corrected pseudo-radial distribution $\tilde{\chi}_1(R)$ for a solution of $[Rb^+:(2\text{-}2\text{-}2)\text{cryptand}]BPh_4^-$ in pyridine (0.15 M) at the rubidium K-edge.

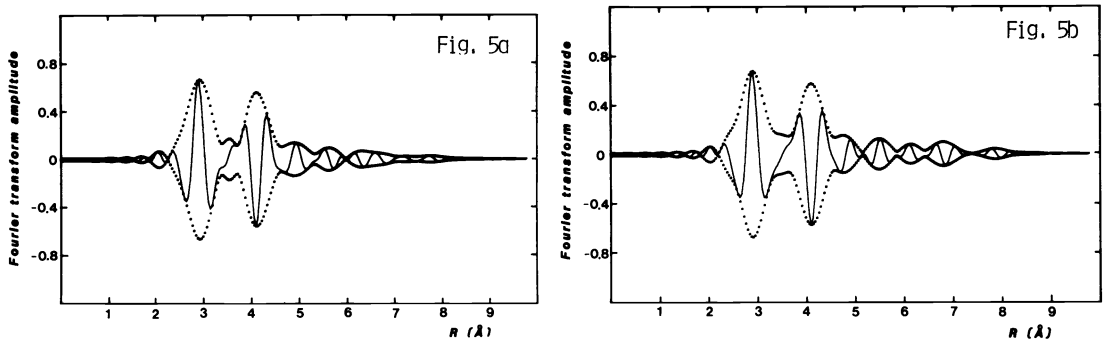

Fig. 5a. EXAFS corrected pseudo-radial distribution $\tilde{\chi}_1(R)$ at the rubidium K-edge for a solution of $[Rb^+:(15\text{-}C\text{-}5)_n]BPh_4^-$ in pyridine, with the ratio r = [ligand]/[ion] equal to 1.8 .

Fig. 5b. EXAFS corrected pseudo-radial distribution $\tilde{\chi}_1(R)$ at the rubidium K-edge for a solution of $[Rb^+:(15\text{-}C\text{-}5)_n]BPh_4^-$ in pyridine, r being equal to 5.6 .

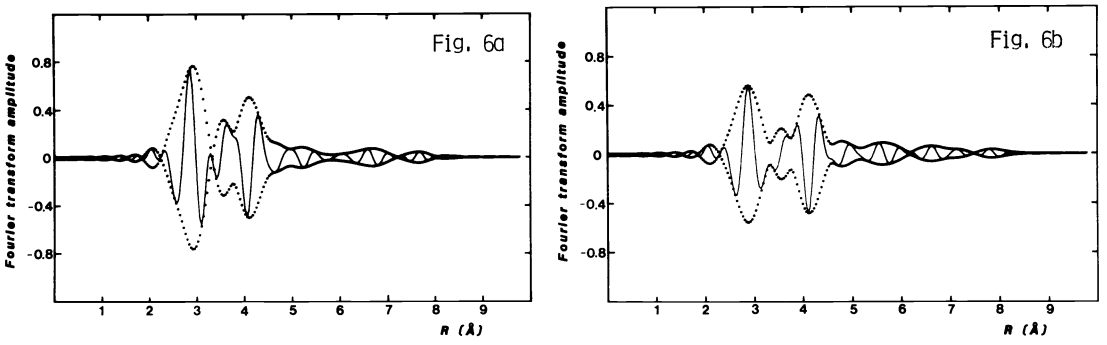

Fig. 6a. EXAFS corrected pseudo-radial distribution $\tilde{\chi}_1(R)$ at the rubidium K-edge for a solution of $[Rb^+:(18\text{-}C\text{-}6)_n]BPh_4^-$ in pyridine (r = 1.1).

Fig. 6b. EXAFS corrected pseudo-radial distribution $\tilde{\chi}_1(R)$ at the rubidium K-edge for a solution of $[Rb^+:(18\text{-}C\text{-}6)_n]BPh_4^-$ in pyridine (r = 6).

If we try now to understand these results, it is essential to remember that the ionic diameter of rubidium (2.94 Å) is too large for this cation to fit into the central cavity of a crown ether (15-C-5) and there are a number of indications (e.g. the solubility of the complex in pyridine requires values of $r \geqslant 2$) that the complexation corresponds to a stoechiometry (1:2). Indeed such (1:2) complexes with 15-C-5 crown ethers have been isolated in the solid state by Truter and coworkers (42), especially with BPh_4^- as counter-ion, and the crystal structure of $[K^+:(\text{benzo-15-C-5})_2]I^-$ (43) gave the first evidence for the reality of the "sandwich" structure first postulated by Pedersen (44). However as observed by Frensdorff (45), it does not necessarily follow that this structure also exists in solution because solvation alters the energetics of the complexing process. Our EXAFS data are definitively not supporting the existence of rigid sandwich complexes in which the cation Rb^+ would be coordinated to 10 oxygen atoms : reference to the data of $[Rb^+:(2\text{-}2\text{-}2)\text{cryptand}]BPh_4^-$ in the same solvent would merely indicate a coordination to about 6 atoms. The EXAFS results would favour the formation of non rigid exclusive dimers as first suggested by Mei, Popov and Dye (46,47) in a determinant work based on ^{133}Cs NMR studies with several macrocyclic ligands. The cation Rb^+ might be coordinated only to three oxygen atoms of each ligand molecule.

A quite similar model would also help to understand our results for the ligand 18-C-6 : obviously on increasing r, we seem to favour the formation of similar dimers, this result being not unexpected if we refer again to the work of Popov and coworkers on $[Cs^+:(\text{dicyclohexyl-18-C-6})_n]BPh_4^-$ in pyridine. On the other hand, the formation of intrinsic complexes for r = 1 seems to be ascertained by a well observable Rb...C shell at 3.8 Å.

The assignment of the strong signal observed at 4.25 Å cannot yet be firmly established. Several interpretations can be formulated but always strong objections are to be raised to them :

(i) An interpretation based on multiple scattering effects would accommodate the inverse phase of the signal and a dense packing of atoms. It is woth noting that in the intrinsic complex $[Rb^+:(2\text{-}2\text{-}2)\text{cryptand}]$, the various multiple scattering paths : $Rb...O_1...O_2...Rb$ ($2R \simeq 8.7$ Å), $Rb...O_1...N_1...Rb$ ($2R \simeq 8.9$ Å), $Rb...O_1...C_1...Rb$ ($7.9 < 2R < 8.3$ Å) and $Rb...C_1...C_2...Rb$ ($2R \simeq 8.9$ Å) fall all in nearly the same range of distances. However, in the EXAFS spectra reproduced in Fig. 4a or Fig. 4b, the amplitude of the signals observed at 4.2 Å is rather small in comparison with the signal of the first shell Rb...O,N : this is not the case for the crown ether solutions and it thus becomes hard to explain why in extrinsic complexes of poor rigidity, multiple scattering signals relative to such long paths could become nearly as intense as the signal of the coordination shell itself, and more intense than the Rb...C shell. On the other hand, we do not imagine a realistic model featuring any colinear arrangement of atoms making a focussing enhancement possible (7).

(ii) There is another hypothesis which would also accommodate such an inverse phase of the signal : the presence at a rather short distance of a heavy scatterer, i.e. another Rb^+ ion. Indeed there is a crystal structure reported in the literature by Dunitz et al. (48) corresponding to dimeric species $[Rb^+:(18\text{-}C\text{-}6),NCS^-]$ where two Rb^+ cations are bridged by NCS^- anions and distant from each other by ~ 5.3 Å . Our attempt to prepare this compound was not quite successful as the EXAFS spectrum did not agree with the predicted structure : the hygroscopic nature of the crown ethers might explain our result. It is however interesting to observe that the latter spectrum looked rather similar to the spectra of the solutions discussed above. This led us to imagine the formation of multimeric species $[Rb^+:(15\text{-}C\text{-}5)_u]_v$ bridged by oxygen atoms, but for Rb-O-Rb angles close to 109°, the calculated distance Rb...Rb should be of the order of 4.75 Å, i.e. significantly larger than our result.

(iii) It is most doubtful that direct interactions between the cation Rb^+ and either the solvent molecules or the anion itself could explain this intense signal at such a large distance. The thermal fluctuations of the distance, i.e. the dynamic disorder of the system, would let any EXAFS oscillation to rapidly vanish. However a static but asymmetric distribution of rigid distances Rb...O and Rb...C might be a reasonable interpretation for a large number of scattering centers. However we do not see how to explain such a rigid distribution of low Z scatterers.

Complexation of strontium ions

The corrected pseudo-radial distributions $\chi_1(R)$ obtained for powdered samples of $[Sr^{2+}:(2\text{-}2\text{-}2)\text{cryptand}],2Br^-$ and $[Sr^{2+}:(18\text{-}C\text{-}6)],2Br^-$ were fully consistent with those of rigid intrinsic complexes with $Sr...O \simeq 2.69$ Å and $Sr...C \simeq 3.78$ Å, whereas a total disruption of the ion pair Sr...Br was observed. Again the EXAFS spectrum of $[Sr^{2+}:(\text{dicyclohexyl-18-C-6})]$, $2Br^-$ in methanol (Fig. 7) seems to exhibit the same amplitude reduction ($\simeq 2/3$), but there is no strong peak at around 4.25 Å. This led us to conclude that only intrinsic complexes (1:1) are present in the solution, with $\bar{N}_1 \simeq 4.5$. For natural ionophores such as the calcimycin (A23187) or the lasalocid (X-537A), we obtained in methanol solution roughly the same mean coordination number (respectively 5.0 and 5.3) suggesting the existence of $[Sr^{2+}:(\text{calcimycin})_2]$ and $[Sr^{2+}:\text{lasalocid}]$ species. However due to the poor rigidity and low symmetry of the carbon backbone, the intensity of the Sr...C signal decreases drastically (Fig. 8).

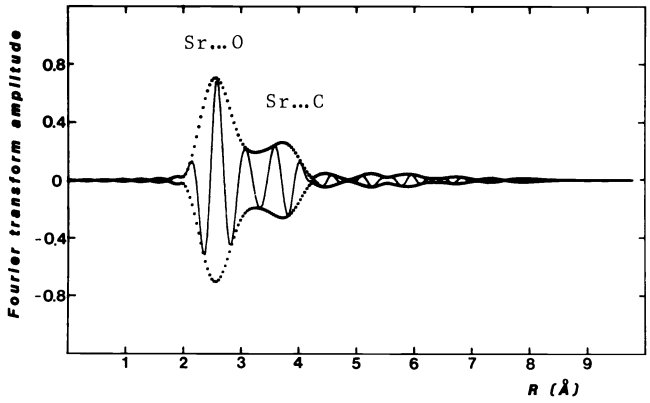

Fig. 7. EXAFS corrected pseudo-radial distribution $\tilde{\chi}_1(R)$ for a solution of $[Sr^{2+}$:(dicyclohexyl-18-C-6)],$2Br^-$ in methanol at the strontium K-edge.

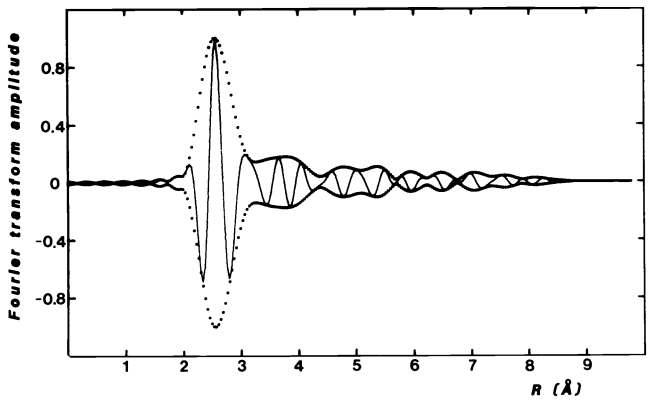

Fig. 8. EXAFS corrected pseudo-radial distribution $\tilde{\chi}_1(R)$ for a solution of $[Sr^{2+}$:lasalocid] in methanol at the strontium K-edge.

CONCLUSION

These various studies clearly indicate that EXAFS psectroscopy should become a very valuable tool for elucidating the structure of aggregates or complexes in non aqueous solutions. However, as illustrated by the case of the solutions of $[Rb^+$:$(15\text{-C-}5)_2]$ in pyridine, the assignment of the various EXAFS contributions is a difficult problem. More work and more beam time will be needed if one plans to establish firmly the origin of the puzzling signal observed at 4.2_5 Å .

Acknowledgements - We wish to thank Dr. P. Lagarde, Dr. D. Raoux and A. Michalowicz for a free access to the EXAFS-I station at LURE. We are indebted to the team of the "Laboratoire de l'Accélérateur Linéaire" (Orsay) for running the DCI machine during dedicated beam time sessions.

REFERENCES

1. B.M. Kincaid and P. Eisenberger, Phys. Rev. Lett. 34, 1361 (1975).
2. R.G. Shulman, P. Eisenberger and B.M. Kincaid, Ann. Rev. Biophys. Bioeng. 7, 559 (1978).
3. S.I. Chan, V.W. Hu and R.C. Gamble, J. Mol. Structure 45, 239 (1978).
4. B.K. Teo, Acc. Chem. Res. 13, 412 (1980).
5. R.G. Shulman, Y. Yafet, P. Eisenberger and W.E. Blumberg, Proc. Nat. Acad. Sci. (USA) 73, 1384 (1976).

6. C.R. Natoli, D.K. Misemer, S. Doniach and F.W. Kutzler, Phys. Rev. A 22, 1104 (1980).
7. B.K. Teo and D.C. Joy, EXAFS Spectroscopy - Techniques and Applications, Plenum Press, New York (1981)
8. R. de L. Kronig, Z. Phys. 70, 317 (1931).
9. E.A. Stern, Phys. Rev. B 10, 3027 (1974).
10. E.A. Stern, D.E. Sayers and F.W. Lytle, Phys. Rev. B 11, 4838 (1975).
11. J. Jaklevic, J. Kirby, M.P. Klein, A. Robertson, G.S. Brown and P. Eisenberger, Solid State Commun. 23, 679 (1977).
12. P. Eisenberger and B. Kincaid, Chem. Phys. Lett. 36, 134 (1975).
13. A. Fontaine, P. Lagarde, D. Raoux, M.P. Fontana, G. Maisano, P. Migliardo and F. Wanderlingh, Phys. Rev. Lett. 41, 504 (1978).
14. D. Sandstrom, J. Chem. Phys. 71, 2381 (1979).
15. A. Fontaine, P. Lagarde, D. Raoux, A. Sadoc and P. Migliardo, J. Chem. Phys. 72, 3061 (1980).
16. P. Rabe, G. Tolkiehn and A. Werner, J. Phys. C 12, 1173 (1979).
17. T.K. Sham, J.B. Hastings and M.L. Perlman, J. Am. Chem. Soc. 102, 5904 (1980).
18. T.K. Sham and B.S. Brunschwig, J. Am. Chem. Soc. 103, 1590 (1981).
19. J.V. Acrivos, K. Hathawa , A. Robertson, A. Thompson and M.P. Klein, J. Phys. Chem. 84, 1206 (1980).
20. A. Sadoc, A. Fontaine, P. Lagarde and D. Raoux, J. Am. Chem. Soc. 103, 6287 (1981).
21. J. Goulon, C. Goulon-Ginet and M. Chabanel, J. Sol. Chem. 10, 649 (1981).
22. B.K. Teo, P.A. Lee, A.L. Simmons, P. Eisenberger and B.M. Kincaid, J. Am. Chem. Soc. 99, 3854 (1977).
23. B. Lengeler and P. Eisenberger, Phys. Rev. B 21, 4507 (1980).
24. J. Goulon, C. Goulon-Ginet, R. Cortes and J.M. Dubois, J. Physique 43, 539 (1982).
25. E.A. Stern, S.M. Heald and B. Bunker, Phys. Rev. Lett. 42, 1372 (1979).
26. P. Lee and G. Beni, Phys. Rev. B 15, 2862 (1977).
27. T.L. Li and G. Stucky, Inorg. Chem. 12, 441 (1973).
28. J.L. Glimois, Thèse de Spécialité, Nantes (1973).
29. A. Verneuil, Ann. Chim. Phys. 6, 294-303 (1886).
30. A.T. Pilipenko and I.P. Serada, Ukrainian Chem. J. 17, 76 (1951) ; Zh. Anal. Khim. 13, 3 (1958) ; Zh. Neorgan. Khim. 6, 413 (1961).
31. D.R. Goddard, B.D. Lodam, S.O. Ajayi and M.J. Campbell, J. Chem. Soc. A, 506 (1969).
32. H. Van Bekkum, J.D. Reminjse and B.M. Wepster, Chem. Commun., 67 (1969).
33. J.J. Rutherford and C.C. Calvo, Beschr. Krist. 128, 229 (1969).
34. M. Bonamico and G. Dessy, J. Chem. Soc. A, 264 (1971).
35. E.V. Khlystunova, I.M. Cheremisina, V.L. Varrand and V.M. Shul'man, Izv. Akad. Nauk. SSSR Khim., 1551 (1971).
36. N.R. Kunchur and M.R. Truter, J. Chem. Soc., 3478 (1958).
37. D.DeW. Hall and W.DeW. Horrocks, Inorg. Chem. 8, 1809 (1969).
38. J.E. O'Connor and E.L. Lamma, Chem. Commun., 892 (1968).
39. T. Yamaguchi and H. Ohtaki, Bull. Chem. Soc. Jpn. 51, 3227 (1978).
40. L.E. Sutton, Tables of Interatomic Distances and Configuration in Molecules and Ions, The Chemical Society, London (1958).
41. J.M. Lehn, Acc. Chem. Res. 11, 49 (1978).
42. D. Moras, B. Metz and R. Weiss, Acta Cryst. B 29, 383 (1973).
43. D.G. Parsons, M.R. Truter and J.N. Wingfield, Inorg. Chim. Acta 14, 45 (1978).
44. P.R. Mallinson and M.R. Truter, J.C.S. Perkins II, 1818 (1972).
45. C.J. Pedersen, J. Am. Chem. Soc. 92, 386 (1970).
46. H.K. Frensdorff, J. Am. Chem. Soc. 93, 600 (1971).
47. E. Mei, A.I. Popov and J.L. Dye, J. Am. Chem. Soc. 99, 6532 (1977).
48. E. Mei, A.I. Popov and J.L. Dye, J. Phys. Chem. 81, 1677 (1977).
49. J.D. Dunitz, M. Dobler, P. Seiler and R.P. Phizackerley, Acta Cryst. B 30, 2733 (1974).